Submitted to the 4th International Conference on Climbing and Walking Robots CLAWAR, Karslruhe, Germany, September 24--26, 2001.

Joystick Force Feedback based on Proximity to the Linearised Workspace of the Four-legged Robot ALDURO

Daniel Germann
Tobias Bruckmann
Manfred Hiller
Mechatronics Laboratory, Gerhard-Mercator-University Duisburg, Germany

ABSTRACT

The aim of this paper is to investigate possibilities for controlling a four-legged walking robot (ALDURO) with a force feedback joystick. A way to filter motion induced errors out of the input data is shown, as well as ways to prevent them by using force feedback. Force feedback can also be used to supply the operator with information about the workspace of ALDURO. A linearised approximation of the workspace of a leg, and a basic approach to extend it to the whole robot are described.

1 INTRODUCTION

The four-legged walking robot ALDURO (Anthropomorphically Legged and Wheeled Duisburg Robot) is being built in the Mechatronics Laboratory at the Gerhard-Mercator-University of Duisburg, Germany, and consists of a 1.8 m by 2.1 m platform with a cabin for the operator, a powerplant and four legs, each 1.6 m long (see fig. 1). Its estimated weight is 1500 kg. The machine will be equipped with a 31 kW diesel engine. The field of possible applications includes excavation, forestry and other tasks in difficult to access terrain. There are two possible configurations, one with four identical legs for manoeuvring in uneven terrain, and a second configuration where the feet of the two hind legs are replaced by wheels, combining the manoeuvrability of legs with the speed and stability of wheels [1].

Figure 1: ALDURO

To simplify the task of steering and control a force feedback joystick was chosen as the interface between operator and robot. The coordination of the actual joints is carried out by an onboard computer. The characteristics of the data transfer operator-joystick-machine, and vice versa, have to be investigated in order to achieve optimal behaviour of the man-machine system (section 2).

When not in walking mode, but executing some other (stationary) task, it would be nice to inform the operator about proximity to the limit of ALDUROs workspace (section 3). Possibilities are acoustic, optical or haptic signals. Because ALDURO is expected to be noisy and the operator has to concentrate on his surroundings, haptic signals using the joystick were chosen.

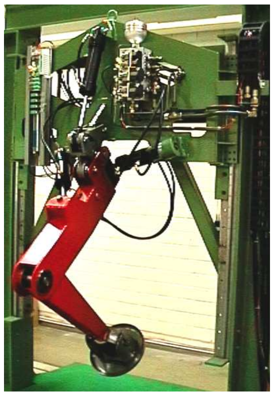

Figure 2: Leg test stand.

To test these concepts we use a single leg test stand, which carries a full scale ALDURO leg on a hip that is free to move in the vertical direction (see fig. 2). The leg is controlled using a commercial force feedback joystick.

2 INTERFACE

With a joystick as the input device for the steering, there are two feasible concepts for describing the desired platform motion: position control and speed control. Being in position control mode, the joystick deflection is interpreted as desired position. This is typical for controlling stationary robots with a limited workspace. In speed control mode, the joystick data is interpreted as desired velocity. Since we have a robot with an non-limited workspace (when walking), speed control makes more sense. This can be compared to driving a car – the accelerator position is proportional to the desired speed. In this case however, we can choose both speed and direction with the joystick.

2.1 Feedforward

During operation the ALDURO driver/operator can be exposed to abrupt movements of the platform. These can be passed to the joystick via the driver's hand, where they will cause unintentional control pulses. To achieve comfortable and safe locomotion this can be reduced by a) fixing an armrest to the joystick and b) software compensation and/or filtering of control pulses.

To reduce small involuntary movements a “virtual spring damper system” between the actual x and y joystick positions and the data used as the control input is introduced. The input data for speed control $\boldsymbol{x}_{control} = [x_{control}, y_{control}]^T$ follows the joystick output data $\boldsymbol{x}_{joystick} = [x_{joystick}, y_{joystick}]^T$ with a spring-damper-system like behaviour (fig. 3). By adjusting spring and damper coefficients, small short movements can be eliminated while large deflections of the joystick are transmitted almost instantly.

With m as mass of the virtual data point $\boldsymbol{x}_{control}$, c as spring and d as damping coefficient, the spring damper system is described by

$$m\ddot{\boldsymbol{x}}_{control} = c\boldsymbol{\Delta x} - d\boldsymbol{\Delta \dot{x}}, \text{ with } \boldsymbol{\Delta x} = \boldsymbol{x}_{joystick} - \boldsymbol{x}_{control}. \quad (1)$$

Substituting $\omega_0 = c/m$ and $\zeta = d/2m$ we get

$$\ddot{\boldsymbol{x}}_{control} - 2\zeta\dot{\boldsymbol{x}}_{control} + \omega_0^2\boldsymbol{x}_{control} = -2\zeta\dot{\boldsymbol{x}}_{joystick} + \omega_0^2\boldsymbol{x}_{joystick}. \tag{2}$$

Eqn. (2) is discretised and integrated during operation to provide the input for the path planner $\boldsymbol{x}_{control}$. By adjusting ω_0 we can influence the frequency of the signals that are filtered. ζ sets the damping characteristics.

2.2 Force Feedback

Force feedback can be used to inform the operator about the state of the robot (workspace, stability). At the same time it can also offer the user assistance for positioning the joystick. To help the driver to find the zero position, an automatic centring feature generates a force that returns the joystick to its centre position.

Another common setting is straight ahead motion. To avoid unintended sideways movements, a force is generated to keep the joystick on the forward axis.

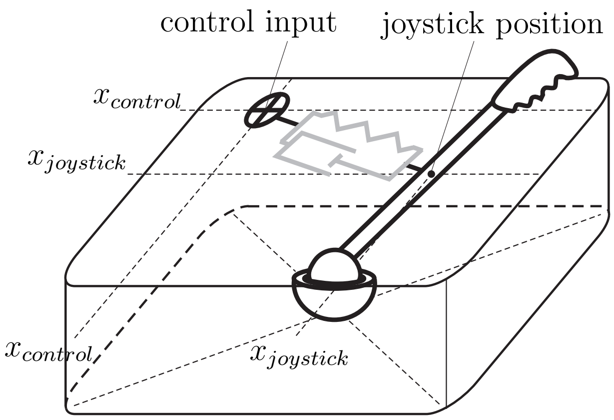

Figure 3: Virtual spring-damper system between actual joystick position and control input.

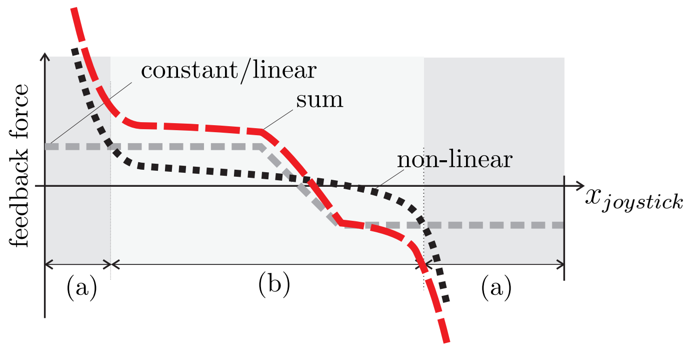

Figure 4: Adding constant/linear device-originating and non-linear kinematics-originating forces.

The feedback forces can be classified into two groups: forces that are joystick based, i.e. depend only on the joystick input data, and forces that describe the state of the robot (workspace, stability) [2]. Workspace as well as stability are only of interest to the operator when the robot is close to the limit. To obtain an optimal blend we choose constant or linear device-originating forces and non-linear kinematics-originating forces for data. Fig. 4 shows an auto-centering force that is dominant in (b) and non-linear force (i.e. information about workspace) dominant in (a).

Because there are only two force feedback axes, three-dimensional data (e.g. force vectors) has to be reduced either by projecting or folding onto the (x, y) plane.

3 WORKSPACE

When ALDURO is carrying out a stationary task, i.e. without moving its feet, it is necessary to know the limits of possible leg joint movements. The workspace of the end-effector – here the platform – with its 16 joints and six degrees of freedom (d.o.f.) is very complex. A first step we will therefore investigate the workspace of a single leg on a fixed platform (see 3.1). The end-effector is the foot. The next step is to look for a way to expand this knowledge from one leg to the platform (see 3.4).

3.1 Linearised Workspace

The human like (anthropomorphic) legs consist of a hip joint with three rotational d.o.f. (ϕ, θ and ψ) and a knee joint with one rotational degree of freedom (ω), actuated by four hydraulic cylinders (see fig. 5).

If we assume the joints are able to rotate 360° around their respective axes we get a maximal workspace for the foot which can be described by a hollow sphere. Its outer radius is the length of the fully stretched leg, and its inner radius the difference between the lengths of thigh and lower leg. This space is limited in reality by the travel of the cylinders. The resulting limited workspace is difficult to describe analytically. Therefore we approach the problem by linearising the workspace at the momentary position of the end-effector. Different analytical approaches are suggested in [3] and [4]. Using a linearised model has the advantage of needing less computational time. As we are not interested in the shape of the workspace itself, but in the momentary proximity to and direction of the limits closest to the end-effector, linearisation is admissible.

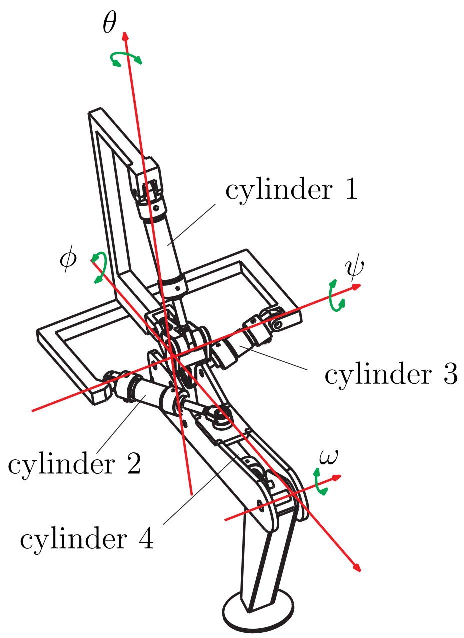

Figure 5: Kinematics of the ALDURO leg.

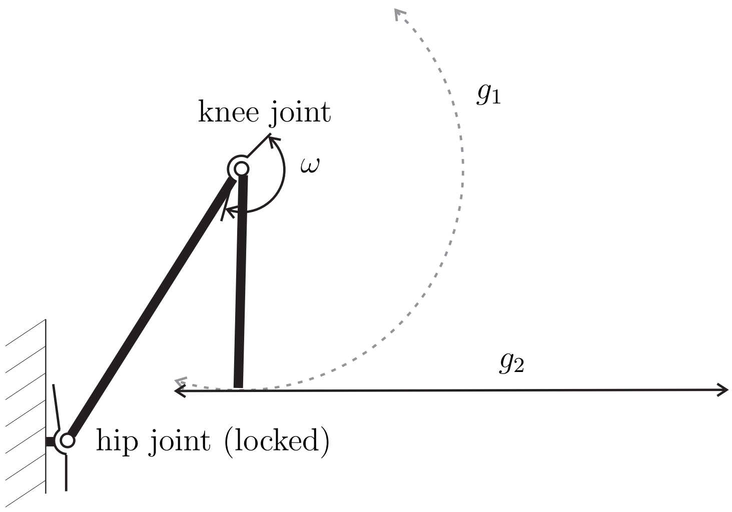

Figure 6: Actual and linearised movement of the end-effector.

The real trajectory g_1 of the end-effector of a one-d.o.f. mechanism can be approximated by its linearised curve g_2 for small movements $\delta\omega$ (see fig. 6). Let $\boldsymbol{q} \in \mathbb{R}^4$ be the vector of the cylinder positions, $\boldsymbol{x} \in \mathbb{R}^3$ the end-effector position, $\boldsymbol{\Phi} : \mathbb{R}^4 \to \mathbb{R}^3$ the known forward kinematics [5] and $\boldsymbol{J} \in \mathbb{R}^{3\times4}$ its Jacobian. Then

$$\boldsymbol{x} = \boldsymbol{\Phi}\left(\boldsymbol{q}\right), \quad \boldsymbol{J} = \frac{\partial \boldsymbol{\Phi}}{\partial \boldsymbol{q}}. \tag{3}$$

With the Jacobian $\boldsymbol{J}$ we can determine the small movement $\delta\boldsymbol{x}$ of the end-effector caused by a small movement $\delta\boldsymbol{q}$ of the cylinders

$$\delta\boldsymbol{x} = \boldsymbol{J} \cdot \delta\boldsymbol{q}. \tag{4}$$

If, instead of taking a small movement δq_i, we take the movements of a cylinder to its left hand end of travel Δq_i^- and right hand end of travel Δq_i^+, we get an approximation of the one-dimensional workspace of the end-effector with only one active cylinder i

$$\boldsymbol{e}_i^- = \Delta q_i^- \boldsymbol{J}^i, \quad \boldsymbol{e}_i^+ = \Delta q_i^+ \boldsymbol{J}^i, \quad \boldsymbol{J}^i = i^{th} \text{ column of } \boldsymbol{J}, \quad i = 1, \ldots, 4\,. \tag{5}$$

Vectors $\boldsymbol{e}_i^-$ and $\boldsymbol{e}_i^+$ are collinear and point in opposite directions. With the four pairs $\{\boldsymbol{e}_i\} = \{\boldsymbol{e}_i^-, \boldsymbol{e}_i^+\}$ we can describe the linearised workspace of the end-effector in the following way: the pairs $\{\boldsymbol{e}_1\}$ and $\{\boldsymbol{e}_2\}$ span a rhombus $\lozenge_{12}$ (fig. 7a), pairs $\{\boldsymbol{e}_1\}$, $\{\boldsymbol{e}_2\}$ and $\{\boldsymbol{e}_3\}$ extend this to form a prism (fig. 7b), and together with pair $\{\boldsymbol{e}_4\}$ a dodecahedron (fig. 7c and fig. 7d), with 14 vertices and 12 rhombi as surface planes.

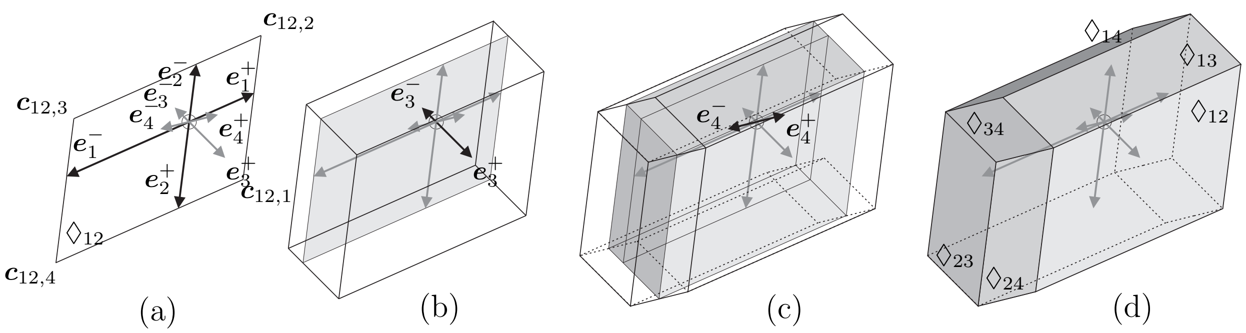

Figure 7: Construction of the linearised workspace.

To obtain these limiting planes, we define the vectors $\hat{\boldsymbol{e}}_i$

$$\hat{\boldsymbol{e}}_i = \lambda_1\, \boldsymbol{e}_i^+ + \lambda_2\, \boldsymbol{e}_i^-, \quad \lambda_1, \lambda_2 \in [0,1], \quad i = 1, \ldots, 4\,. \tag{6}$$

Setting two of the vectors $\hat{\boldsymbol{e}}_i$ and $\hat{\boldsymbol{e}}_j$ to one of their two extrema ($\boldsymbol{e}_i^-$ or $\boldsymbol{e}_i^+$, and $\boldsymbol{e}_i^-$ or $\boldsymbol{e}_i^+$ respectively) and combining them we get four vertices (fig. 7a) with vectors $\boldsymbol{c}_{ij,k}$, k=1,. . . ,4

$$\begin{aligned}
\boldsymbol{c}_{ij,1} &= \boldsymbol{e}_i^+ + \boldsymbol{e}_j^+,\\
\boldsymbol{c}_{ij,2} &= \boldsymbol{e}_i^+ + \boldsymbol{e}_j^-,\\
\boldsymbol{c}_{ij,3} &= \boldsymbol{e}_i^- + \boldsymbol{e}_j^-,\\
\boldsymbol{c}_{ij,4} &= \boldsymbol{e}_i^- + \boldsymbol{e}_j^+, \quad i < j, \quad i, j = 1, \ldots, 4\,.
\end{aligned} \tag{7}$$

At each vertex the two remaining vector pairs $\{\boldsymbol{e}_m\}$, $\{\boldsymbol{e}_n\}$, $i, j \neq m, n$ span the rhombus $\lozenge_{mn,k}$ with normal vector $\boldsymbol{n}_{mn,k}$ and distance $d_{mn,k}$ to the end-effector,

$$\boldsymbol{n}_{mn,k} = \frac{\hat{\boldsymbol{e}}_m \times \hat{\boldsymbol{e}}_n}{|\hat{\boldsymbol{e}}_m \times \hat{\boldsymbol{e}}_n|}, \tag{8}$$

$$d_{mn,k} = \boldsymbol{c}_{ij,k} \cdot \boldsymbol{n}_{mn,k}, \quad i < j, \quad m < n, \quad i, j \neq m, n, \quad i, j, m, n, k = 1, \ldots, 4\,. \tag{9}$$

The two rhombi closer to the end-effector are inside the workspace and the other two are the limiting planes. These two limiting planes are always on opposite vertices, $\boldsymbol{c}_{ij,1}$ and $\boldsymbol{c}_{ij,3}$, or $\boldsymbol{c}_{ij,2}$ and $\boldsymbol{c}_{ij,4}$.

The vector $\boldsymbol{c}_{ij,k}$ is made up of two parts (eqn. 7). The components of these two parts in direction of $\boldsymbol{n}_{mn,k}$ must have the same sign for the plane to be as far away as possible from the end-effector. When $\boldsymbol{e}_i^+ \cdot \boldsymbol{n}_{mn,1}$ and $\boldsymbol{e}_j^+ \cdot \boldsymbol{n}_{mn,1}$ have the same sign then the rhombi $\Diamond_{mn,1}$ and $\Diamond_{mn,3}$ are the limiting planes, otherwise $\Diamond_{mn,2}$ and $\Diamond_{mn,4}$ are the limiting planes. Thus the distances to the two outer planes are

$$d_{mn}^- = \begin{cases} d_{mn,1} & \text{for} \quad s > 0 \\ d_{mn,2} & \text{for} \quad s \leq 0 \end{cases} \tag{10}$$

$$d_{mn}^+ = \begin{cases} d_{mn,3} & \text{for} \quad s > 0 \\ d_{mn,4} & \text{for} \quad s \leq 0 \end{cases}, \qquad s = \operatorname{sgn}(\boldsymbol{e}_i^+ \cdot \boldsymbol{n}_{mn,1}) \operatorname{sgn}(\boldsymbol{e}_j^+ \cdot \boldsymbol{n}_{mn,1}), \quad m < n\,. \tag{11}$$

As there are four pairs of vectors $\{\boldsymbol{e}_i\}$ there are only six possibilities for combining them to form a plane $\Diamond_{mn,k}$. This gives us the 12 planes to close our workspace.

3.2 Repulsive Force

The motivation for determining the workspace is to inform the operator of the proximity of its limits. As it is inconvenient to feed back to the operator all directions and distances to all limiting planes they are merged into one value. Each limiting plane exerts a force on the end-effector, pushing it away. The magnitude of this force is a function of the distance between plane and end-effector. The closer a plane is, the bigger the force. A non-linear relation is chosen:

$$\boldsymbol{f}_{mn}^k = -\operatorname{sgn}(d_{mn}^k) \cdot \boldsymbol{n}_{mn} \cdot C_1 \cdot C_2^{|d_{mn}^k|}, \quad k = -,+, \quad m < n, \quad C_2 \in (0,1)\,, \tag{12}$$

where C_1 is a proportional factor.

This is also the reason for the admissibility of the linearisation: The error for planes (i.e. limits) close to the end-effector is small, but their influence on the repulsive force is strong. For limits far away the error of linearisation is huge, but their influence is negligible.

The sum $\boldsymbol{f}$ of the repulsive forces of all limiting planes (i.e. limits of the cylinders) is then fed back to the operator

$$\boldsymbol{f} = \sum_{\substack{m,n=1 \\ m<n}}^{4} \boldsymbol{f}_{mn}^+ + \boldsymbol{f}_{mn}^-. \tag{13}$$

3.3 Example

This scheme has been implemented in MATLAB and will be transferred to the leg test stand, where it will be integrated in the force feedback concept.

As an example we shall demonstrate the calculation of the workspace. For the cylinder positions $\boldsymbol{q} = [0.15875, 0.10656, 0.08319, 0.04366]^T$ the resulting end-effector position is $\boldsymbol{x} = [0.2756, -0.1561, -1.2383]^T$. The Jacobian $\boldsymbol{J}$ projects the differences between the actual cylinder positions to their respective ends of travel into the vector pairs $\{\boldsymbol{e}_1^-, \boldsymbol{e}_1^+\}$ to $\{\boldsymbol{e}_4^-, \boldsymbol{e}_4^+\}$ (see fig. 8). Pairs 1 and 4 are the longest as they originate from the main hip and knee movement. The combination of all four pairs results in a workspace limited by

12 planes (see fig. 9). The resulting force $\boldsymbol{f}$ in fig. 8 is pointing downwards. The reason for that is that the knee cylinder – the only one to provide an upwards movement – is close to its end of travel.

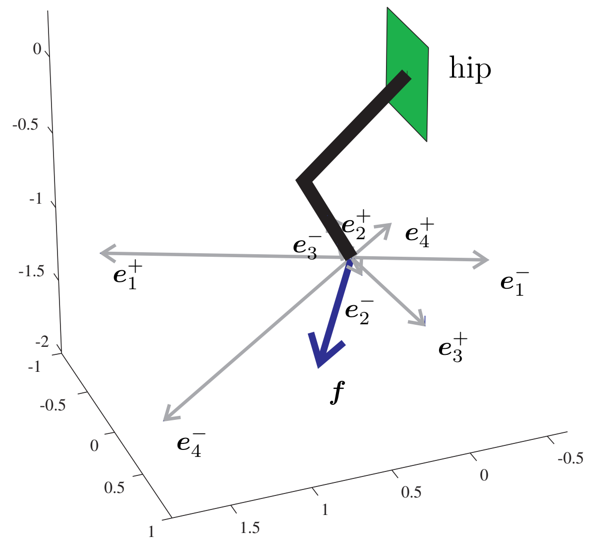

Figure 8: Vector pairs $\{\boldsymbol{e}_1\}$ to $\{\boldsymbol{e}_4\}$ and resulting repulsive force $\boldsymbol{f}$

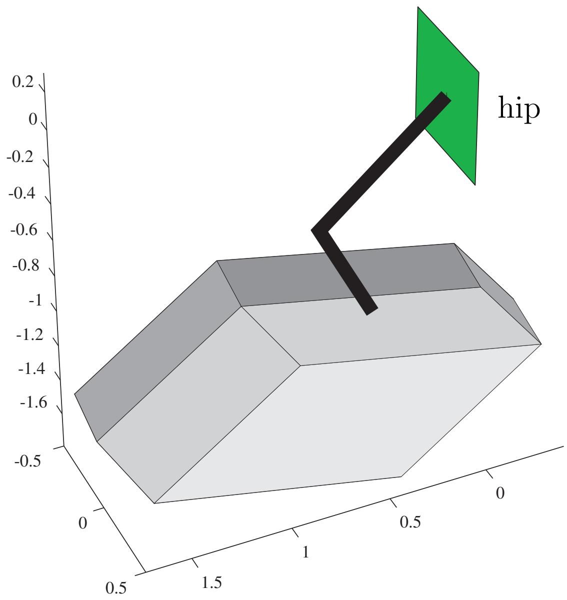

Figure 9: Linearised workspace (dodecahedron) scaled by 0.5.

3.4 Platform Workspace

The aim of this subsection is to show how to extend this principle from one leg to the platform.

The movements that are of primary interest for ALDURO when in stationary operating mode are a) translations in all three directions and b) rotations around an axis perpendicular to the platform. They are to be treated separately.

If only translational movements of the platform are allowed, all four connecting points (i.e. hip joints) to the legs move identically with no rotational component. Having a fixed foot point and a hip that is free to move translationally instead of a fixed hip and the foot as end-effector (see 3.1) results in the same workspace with opposite signs. The workspace for the center of the platform is the intersection of the four workspaces translated to the center.

To examine the platforms ability to turn around its vertical axis all d.o.f. except the one around the vertical axis are locked. A clockwise rotation of the platform is identical to a counterclockwise rotation of all four feet. Further investigation and tests are needed to show if it is admissible to describe the workspace for vertical rotation as the intersection of rotational movements of the feet within their respective workspaces.

4 CONCLUSION

The force feedback joystick offers a suitable interface for the steering and control of the four-legged walking robot. A simple method for filtering unintentional movement from the joystick input data has been presented. For evaluation it will be benchmarked with classical filtering methods (e.g. Butterworth filter).

Its force feedback capability can be used to assist the driver with his movements, as well as informing him on the proximity of the limits of workspace by means of a repulsive force. A way to calculate the linearised workspace of one leg has been presented and is being tested on the test stand. Future work will expand this to the workspace of the platform.

References

[1] M. Hiller, J. Müller, U. Roll, M. Schneider, D. Schröter, M. Torlo, and D. Ward. The mechatronic design and development of the mobile robot ALDURO. In *Proceedings of the IARP Workshop on biologically motivated service robotics*, Jena, Germany, June 21–23 1999.

[2] Xunzhang Wang, Gerald G. L. Seet, Michael W. S. Lau, Eicher Low, and K. C. Tan. Exploiting force feedback in pilot training and control of an underwater robotics vehicle: an implementation in LabVIEW. In *Oceans Conference Record (IEEE)*, volume 3, pages 2037–2042, Piscataway, NJ, USA, September 11–14 2000.

[3] K. Abdel-Malek, H.J. Yeh, and S. Othman. Interior and exterior boundaries to the workspace of mechanical manipulators. In *Robotics & Computer-Integrated Manufacturing*, volume 16, pages 365–376, October 2000.

[4] M. Ceccarelli and A. Vinciguerra. On the workspace of general 4R manipulators. In *International Journal of Robotics Research*, volume 14, pages 152–160, 2 April 1995.

[5] J. Müller, M. Schneider, and M. Hiller. Modelling and simulation of the large-scale hydraulically driven ALDURO. In *Proceedings of the Euromech Colloquium 375*, pages 116–123, Munich, Germany, March 23–25 1998.